British Journal of Cancer www.nature.com/bjc

ARTICLE

Translational Therapeutics

Preclinical study of ^{212}Pb alpha-radioimmunotherapy targeting CD20 in non-Hodgkin lymphoma

Stéphanie Durand-Panteix[1], Jacques Monteil[1,2], Magali Sage[1], Armand Garot[2], Marie Clavel[1], Amal Saidi[3], Julien Torgue[3], Michel Cogne[1]✉ and Isabelle Quelven[1,2,4]✉

BACKGROUND: Despite therapeutic advances, Non-Hodgkin lymphoma (NHL) relapses can occur. The development of radioimmunotherapy (RIT) with α-emitters is an attractive alternative. In this study, we investigated the potential of α-RIT in conjunction with ^{212}Pb-rituximab for the treatment of NHL.
METHODS: EL4-hCD20-Luc cells (mouse lymphoma cell line) were used for in vitro and in vivo studies. Biodistribution and efficacy studies were performed on C57BL/6 mice injected intravenously with 25×10^3 cells.
RESULTS: ^{212}Pb-rituximab (0.925–7.4 kBq/mL) inhibit proliferation of EL4-hCD20-Luc cells in vitro. Biodistribution of $^{203/212}$Pb-rituximab in mice showed a significant tumour uptake and suggested that the liver, spleen, and kidneys were the organs at risk. For efficacy studies, mice were treated at either 11 days (early stage) or 20–30 days after injection of tumour cells (late stage). Treatment with 277.5 kBq ^{212}Pb-rituximab significantly prolonged survival. Even at an advanced tumour stage, significant tumour regression occurred, with an increase in the median survival time to 28 days, compared with 9 days in the controls.
CONCLUSIONS: These results show the efficacy of ^{212}Pb-rituximab in a murine syngeneic lymphoma model, in terms of significant tumour regression and increased survival, thereby highlighting the potency of α-RIT for the treatment of NHL.

British Journal of Cancer; https://doi.org/10.1038/s41416-021-01585-6

BACKGROUND

Non-Hodgkin lymphoma (NHL) accounts for over 85% of lymphoma cases, and it is the eighth most commonly diagnosed cancer in men and the eleventh in women worldwide [1]. The addition of an anti-cluster of differentiation 20 (CD20) monoclonal antibody (mAb) to therapeutic armamentarium has been one of the most important developments in NHL treatment during the last 30 years. Rituximab was the first mAb to be approved for the treatment of NHL and has become a mainstay in therapy for a broad range of B-cell malignancies [2]. Despite significantly improved response and survival rates, many patients relapse. Radioimmunotherapy (RIT) is a promising second-line option. Two anti-CD20 mAbs coupled with β-emitters, ^{90}Y-ibritumomab tiuxetan (Zevalin®) and ^{131}I-tositumomab (Bexxar®), have been developed and approved by the U.S. Food and Drug Administration (FDA) [3]. Despite favourable results for the treatment of low-grade NHL, most patients with aggressive or relapsed/refractory NHL relapse after RIT. Novel methods that improve the efficiency of RIT and reduce its toxicity are needed [4].

The development of RIT with α-emitters is an attractive therapeutic alternative [5], particularly for haematological malignancies [6]. α-particles provide a short path length of 50–80 µm in tissues, compared with a few millimetres with β-particles, reducing the unwanted radiation exposure of normal tissues, thereby representing a good solution for small or disseminated tumours. Furthermore, α-particles produce clustered DNA double-stranded breaks and highly reactive hydroxyl radicals when traversing biological tissues. Considering their high linear energy transfer of 50–230 keV/µm, α-emitters have 100-fold higher cytotoxicity compared with β-emitters (0.1–1.0 keV/µm). These two properties result in higher tumour cell killing and lower toxicity to surrounding tissues. The cytotoxicity of α-particles is independent of both the dose rate and the oxygenation status of cells. Only a few α-emitters are considered suitable for therapeutic use in cancer patients. The most studied α-emitters in preclinical or clinical studies are ^{225}Ac ($t_{1/2} = 10$ days), ^{211}At ($t_{1/2} = 7.2$ h), ^{212}Bi ($t_{1/2} = 60.6$ min), ^{213}Bi ($t_{1/2} = 45.6$ min), ^{223}Ra ($t_{1/2} = 11.4$ days), ^{227}Th ($t_{1/2} = 18.7$ days) and ^{149}Tb ($t_{1/2} = 4{,}1$ h), as well as ^{212}Pb ($t_{1/2} = 10.6$ h), a parent of an α-emitter [7, 8]. When selecting a radionuclide, the physical and chemical characteristics, as well as availability, must be considered. ^{212}Pb is a good choice in terms of those aspects. In fact, this radioelement is available at high purity using a ^{224}Ra/^{212}Pb generator. After administration, ^{212}Pb (β-emitter) generates ^{212}Bi (α-emitter); thus, ^{212}Pb, which has an intermediate half-life and is, therefore, relatively convenient for mAb pharmacokinetics, serves as an in vivo α-emitter generator [9]. A macrocyclic bifunctional ligand,

[1]CNRS-UMR7276 – INSERM U1262, Contrôle de la réponse immune B et lymphoprolifération, Limoges University, Limoges, France. [2]Nuclear Medicine Department, Limoges University Hospital, Limoges, France. [3]Orano Med SAS, Paris, France. [4]ToNIC, Toulouse NeuroImaging Center - INSERM U1214, Toulouse, France. ✉email: michel.cogne@inserm.fr; quelven-bertin.i@chu-toulouse.fr

Received: 28 March 2021 Revised: 11 September 2021 Accepted: 4 October 2021
Published online: 20 October 2021

2-(4-isothiocyanotobenzyl)-1,4,7,10-tetraaza-1,4,7,10-tetra-(2-carbamoylmethyl) cyclododecane (4-NCS-Bz-TCMC), was designed and synthesised to obtain greater in vivo stability for the chelation of lead isotopes [10]. mAbs can be easily functionalized with a bifunctional TCMC ligand and then radiolabeled with Pb [10]. Thus, ^{212}Pb has been used to radiolabel anti-CD38 mAbs and showed efficacy in vivo in a mouse myeloma xenograft model [11]. Furthermore, ^{212}Pb was first used in a trial of ^{212}Pb-TCMC–trastuzumab for patients with human epidermal growth factor receptor 2-expressing malignancies [12, 13].

In this study, we developed α-RIT for NHL treatment. We labelled a specific antibody, rituximab, and an isotypic control with ^{212}Pb using the chelating agent TCMC. ^{212}Pb-rituximab was tested in vitro in EL4-hCD20 cells and in vivo in a murine syngeneic lymphoma model based on the same cell line. The biodistribution, toxicity, and efficacy were evaluated to determine the therapeutic potential and safety of this novel RIT strategy.

METHODS

Cell lines, antibodies, and mice

The murine EL4-hCD20-luc lymphoma cell line [14] was maintained in supplemented RPMI 1640 medium. CD20 expression was verified by flow cytometry (Accuri® C6; BD Biosciences, Franklin Lakes, NJ, USA) and bioluminescence imaging (BLI) (IVIS® Lumina LT III; PerkinElmer, Waltham, MA, USA). Rituximab, a mouse/human chimeric mAb (IgG1/kappa) against human CD20, was purchased from Roche (Bâle, Switzerland). For the IgG isotypic control, palivizumab (AbbVie, North Chicago, IL, USA), a humanised mouse mAb (IgG1/kappa) against an epitope of the F protein of respiratory syncytial virus was used. C57BL/6 mice (female, 7–10 weeks) were purchased from Janvier Labs (Le Genest-Saint-Isle, Mayenne, France).

Tumour model

C57BL/6 mice (8 weeks old) were injected intravenously in the tail with 25×10^3 EL4-hCD20-luc cells (in 100 µL phosphate-buffered saline [PBS]). Mice were monitored daily for signs of pain or discomfort and three times a week to evaluate and grade facial expressions of pain [15], behaviour, hair coat scruffiness, weight loss, tumour, and mobility. BLI was performed twice a week after 15–20 days (appearance of detectable tumour). Biodistribution experiments were performed 25 days after engraftment. RIT was performed either 11 days post-engraftment or once the tumour was detectable by BLI (20–30 days post-engraftment). Independent groups of animals were used for the different studies. All in vivo experiments were performed in accordance with animal ethics legislation, and all efforts were made to minimise suffering e.g., by adding nutritional hydrogel. Animals sample size were chosen to minimise the number of animals used in accordance with ethical rules and to respect the principal of the 3Rs. The protocol was approved by the national agency of research (Ministère de l'Enseignement Supérieur, de la Recherche et de l'Innovation - APAFIS#15900-201807061621591 v2).

In vivo BLI

Before in vivo BLI, mice were anaesthetised by isoflurane inhalation and then shaven as well as depilated on the ventral and dorsal faces. The mice were injected with 2 mg VivoGlo™ luciferin (Promega, Madison, WI, USA). Imaging was performed 11 min post-injection using the IVIS® Lumina LT III in vivo imaging system (PerkinElmer) with a binning factor of 16 and an automatic exposure time. Living Image® 4.5 software (PerkinElmer) was used to analyse the signal intensities in longitudinal studies. The different acquisitions were normalised on the same scale.

mAb conjugation and radiolabeling

The two IgGs were conjugated to a customised bifunctional version of TCMC (Macrocyclics, Plano, TX, USA), using an enzymatic procedure based on Jeger et al. [16] and Dennler et al. [17], resulting in up to two TCMC molecules conjugated to a specific amino acid in the Fc portion of the antibody. An in vitro stability study in serum up to 72 h at 37 °C demonstrated >96% remains associated with the chelate; this stability is consistent with that reported for ^{203}Pb using the same chelating agent in Chappell et al. [10]. ^{212}Pb was produced using ^{224}Ra generators provided by Orano Med SAS (Bessines-sur-Gartempes, Haute-Vienne, France). Chelation was performed by incubating with 0.1 or 1 mg mAb-TCMC per 40 MBq ^{212}Pb for 15 min at 37 °C in 150 mM ammonium acetate, pH 4.5. Radiochemical purity, assayed by instant thin-layer chromatography, was >94%. All experiments were performed using a specific activity of 37 MBq/mg, except for the early tumour stage RIT experiments, which were performed at both 37 MBq/mg and 370 MBq/mg. The immunoreactivity of ^{212}Pb-anti-CD20 was assessed in vitroby direct binding assays conducted in EL4-hCD20 cells [18], and a K_D of 12.6 ± 5.8 nM was obtained, consistent with the known affinity of rituximab (K_D = 5.2–11.0 nM) [19]. Furthermore, an immunoreactive fraction >81% was obtained. For single-photon emission computed tomography (SPECT/CT) imaging, mAbs were radiolabeled with ^{203}Pb in 0.5 M HCl (Lantheus Medical Imaging; North Billerica, MA, USA). After adjusting the pH of the ^{203}Pb solution to 4.5 using 1.5 M ammonium acetate, mAbs were incubated for 15 min with ^{203}Pb at 37 °C. The radiochemical purity was >98%, and the specific activity was ~37 MBq/mg.

In vitro studies

Cell proliferation assays were performed using Cell Titer Glo (Promega). EL4-hCD20-luc cells were cultured at 37 °C in 96-well plates (25,000 cells in 100 µL/well), and proliferation was assessed on days 1, 2, and 3 after treatment with various concentrations of ^{212}Pb-MAb (0.925, 1.85, 3.7, and 7.4 kBq/mL) or cold Ab (25–200 ng/mL). The number of viable cells was determined (in triplicate) by measuring the absorbance at 490 nm after the addition of a tetrazolium salt for 2 h. Apoptosis was evaluated using Annexin/7AAD dual staining (BD Pharmingen, San Diego, CA, USA) followed by flow cytometry (Accuri C6; BD Biosciences). The proportion of apoptotic cells included early apoptotic cells (Annexin V^+/$7AAD^-$), late apoptotic cells (Annexin V^+/$7AAD^+$), and necrotic cells (Annexin V^-/$7AAD^+$). All in vitro experiments were performed at least three times.

Biodistribution and SPECT/CT imaging

Biodistribution experiments were performed in tumour-bearing mice at 25 days after engraftment. ^{212}Pb-rituximab or ^{212}Pb-isotypic control (1.85 MBq) was injected intravenously. At each time point (2, 6, 18, 24, or 48 h post-injection), animals having received ^{212}Pb-rituximab (4–5 animals/group) or ^{212}Pb-isotypic control (2–3 animals/group) were euthanized under isoflurane inhalational anaesthesia by cervical dislocation. BLI was performed 1 day before injection and before sacrifice. Selected tissues were excised and weighed. One femur was counted directly and the other one was extracted and flushed to isolate bone marrow. Tissues radioactivity levels were measured using a calibrated γ-counter (PerkinElmer) with an energy window of 190–290 keV considering ^{212}Pb major emitted gamma (238 keV). Radioactivity uptake in the organs was expressed as the percentage injected dose per gram of tissue (%ID/g) after correcting for radioactive decay at each time point. For SPECT/CT imaging, animals were injected with ^{203}Pb-rituximab (18.5–25 MBq) and imaged under isoflurane inhalational anaesthesia (1.8%, 50% air/50% oxygen, 1.4 L/min) at 6, 24, 48, and 96 h after injection using a MicroSPECT/CT (U-SPECT4/CT; MILabs, Utrecht, The Netherlands) and euthanized at the end of experiment to confirm tumoral presence. Image acquisition lasted 30 min for earlier time points to 90 min for later time points. Energy windows were set over the 279 keV peaks (±20%), and a GP-RM collimator was used (75 holes of 1.5 mm diameter, iterative reconstruction OS-EM, no filter −16 subsets/6 iterations/voxel size: 0.8 mm). The SPECT resolution for ^{203}Pb is estimated to be less than 1 mm [20]. Images were analysed with PMOD Software (PMOD Technologies, Zurich, Switzerland).

Dose range finding and toxicity studies

Toxicity studies were conducted in healthy 8-week-old C57BL/6 mice at 7 days, 21 days, or 3 months. Mice received ^{212}Pb-rituximab (185–740 kBq) (7–10/group) by intravenous injection and were compared with mice (5/group) that received PBS, rituximab, isotypic control (100 µg), or 277.5 or 555 kBq ^{212}Pb-isotypic control. Mice were monitored daily and weighed throughout the experiments. Blood was collected at the time of sacrifice (7 days, 21 days, or 3 months). The haemoglobin concentration, white blood cell count, and platelet count were determined using an automated hematology analyzer (Cell Dyn, Abbott Laboratories, Chicago, IL, USA). Biochemical parameters (aspartate amino transferase, alanine amino transferase, urea, and creatinine) were measured in plasma using an automated biochemical analyzer (Konelab, Thermo Fisher Scientific, Waltham, MA, USA).

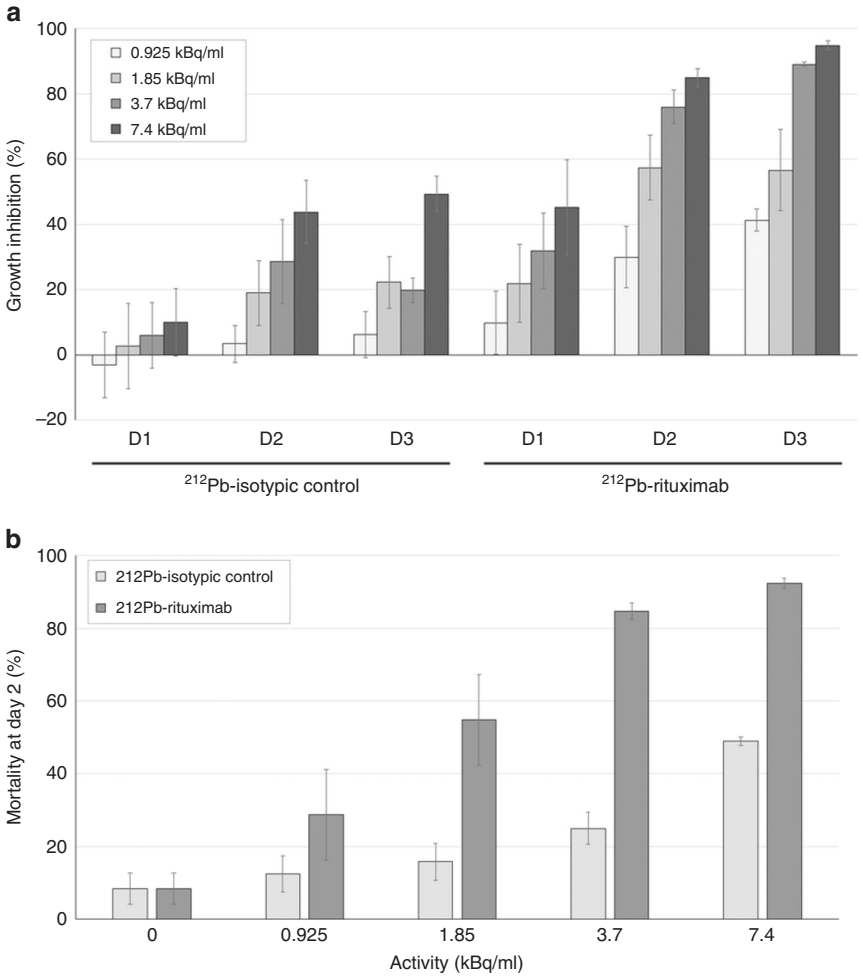

Fig. 1 In vitro studies. Percentage of growth inhibition (**a**) and mortality (**b**) for increasing ^{212}Pb-mAb activity (0.925–7.4 kBq/mL). **a** EL4-hCD20-luc cell growth inhibition percent was calculated, from days 1 to 3, using untreated cells as controls on the same day. Data are expressed as the mean ± SEM percentage of growth inhibition $((1 - OD_{treatment} / OD_{control}) * 100)$. **b** Mortality was evaluated on day 2 by flow cytometry using Annexin V/7AAD dual staining to evaluate early apoptotic, late apoptotic, and necrotic cells.

Radioimmunotherapy studies

Treatment was injected 11 days after intravenous injection of EL4-hCD20-luc cells, or once the tumours were detectable by BLI (20–30 days post-injection). After 11 days, mice post-engraftment (early tumour stage) were randomly assigned to experimental groups (16 mice/group) and received a single intravenous injection of ^{212}Pb-rituximab (277.5 kBq) with a specific activity of 370 or 37 kBq/mg, ^{212}Pb-isotypic control (277.5 kBq, 37 kBq/mg), PBS, or rituximab (40 mg/kg). Mice were monitored daily for general clinical signs and were weighed twice a week. Mice were euthanized when they reached their body weight limit (30% below their weight at day 0) or their general status declined, or if tumour progression caused obvious discomfort, as required by the institutional animal care guidelines. Overall survival was measured as an indicator of therapeutic efficacy. For BLI-detectable tumours (late tumour stage), mice were randomly assigned to experimental groups and received a single intravenous injection of ^{212}Pb-rituximab (277.5 kBq, 37 kBq/mg, $n = 25$), ^{212}Pb-isotypic control (277.5 kBq, 37 kBq/mg, $n = 7$), PBS ($n = 12$), or rituximab (40 mg/kg, $n = 7$), or two injections of ^{212}Pb-rituximab (277.5 kBq, 37 kBq/mg) on days 0 and 7 ($n = 9$) or days 0 and 14 ($n = 11$). The general condition of the mice was monitored, and tumour evolution was assessed by BLI before and after treatment.

Statistical methods

GraphPad Prism v6 (La Jolla, USA) was used to calculate statistical parameters. All p values are two sided and difference were considered significant for $p < 0.05$. In-text numbers indicate means of pooled data ± standard deviation (SD) for biodistribution studies and means ± standard error of the mean (SEM) for other studies. For comparison between treatment at the different analysis time (in vitro studies, biodistribution in tumours and blood toxicity studies), two-way analysis of variance were performed. For RIT studies, survival rates were determined by the Kaplan–Meier method and compared using the log-rank test.

RESULTS

In vitro studies

EL4-hCD20-luc cells were treated with increasing activities (0.925–7.4 kBq/mL) of ^{212}Pb-rituximab or ^{212}Pb-isotypic control. Evaluation of cell proliferation for 3 days showed dose-dependent growth inhibition after ^{212}Pb-rituximab treatment (Fig. 1a). From day 1 and at all activities tested, this inhibition was significantly higher than that induced by the ^{212}Pb-isotypic control ($p < 0.0001$). Similarly, starting at 1.85 kBq/mL, mortality on day 2 was significantly higher ($p < 0.01$) after ^{212}Pb-rituximab treatment than after ^{212}Pb-isotypic control treatment at the same activity (Fig. 1b). The same experiment with increasing concentrations (25–200 ng/mL) of the two cold mAbs, rituximab and isotypic control, showed no significant effects on growth inhibition or mortality (data not shown).

Biodistribution and SPECT-CT imaging of healthy and tumour-bearing mice

The biodistribution of ^{212}Pb-rituximab was evaluated in tumour-bearing mice and compared with ^{212}Pb-isotypic controls to

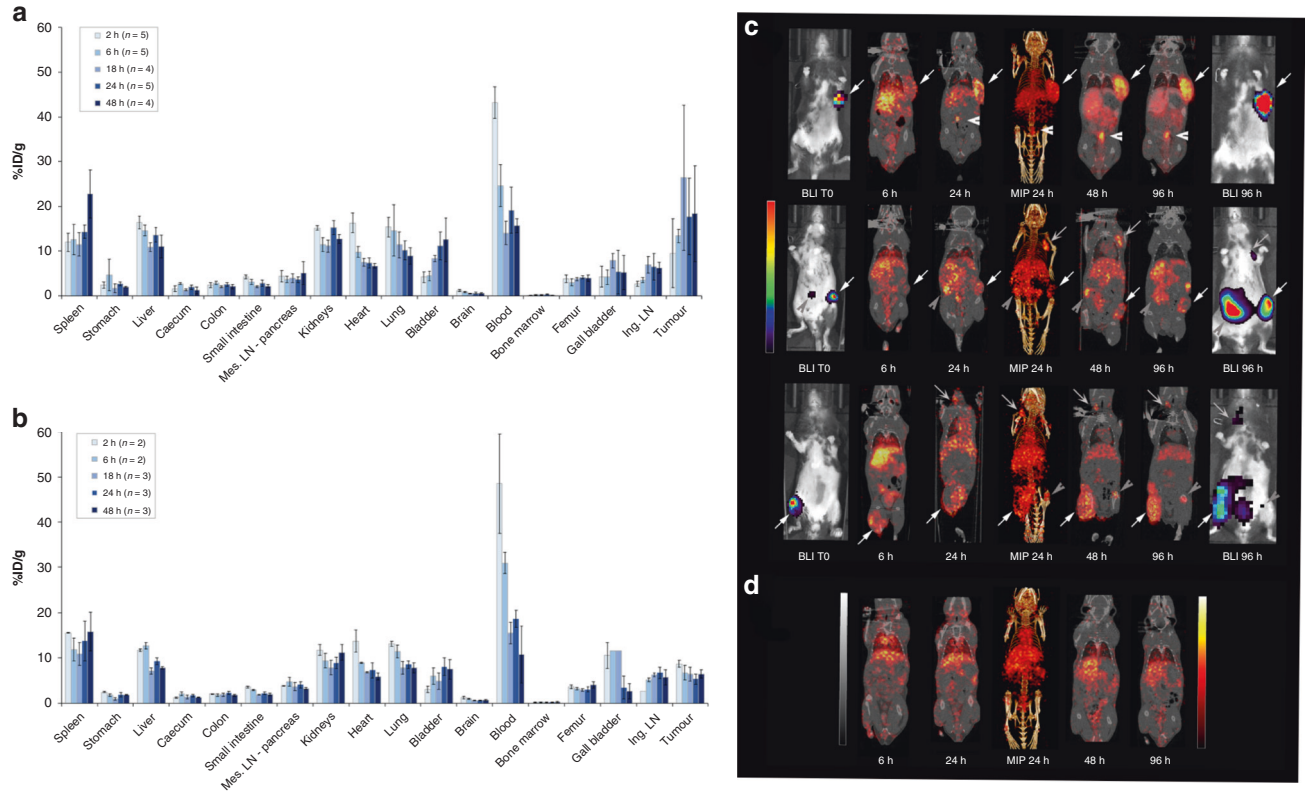

Fig. 2 Biodistribution and SPECT-CT imaging. Biodistribution of ^{212}Pb-rituximab (**a**) and the ^{212}Pb-isotypic control (**b**) in tumour-bearing mice. Mice were injected with 185 kBq ^{212}Pb-mAbs and then sacrificed at 2, 6, 18, 24, or 48 h post-injection. Radioactivity in tumours, organs, and blood was expressed as the mean ± SD percentage injected dose per gram of tissue (%ID/g). In tumours, two-way analysis of variance showed a significant difference between the two mAbs ($p < 0.006$). In vivo imaging of ^{203}Pb-rituximab in tumour-bearing mice (**c**) and healthy mice (**d**). ^{203}Pb-rituximab at 18.5–25 MBq was injected. Mice were imaged by MicroSPECT/CT at 6, 24, 48, and 96 h after injection. For mice bearing tumours (25 days after engraftment), BLI was performed before injection of ^{203}Pb-rituximab and after the last MicroSPECT/CT acquisition. Each line represents the same mouse imaged at different times. Tumours are indicated by different arrows, allowing monitoring of tumour uptake at the same site. Tumoral presence was confirmed post-mortem at the end of experiment.

monitor rituximab tumour CD20+-specific targeting (Fig. 2). After 212Pb-rituximab injection, radioactivity in tumours was 13.4 ± 0.3% ID/g at 6 h and increased over time, persisting at 48 h post-injection 18.4 ± 10.7%ID/g (Fig. 2a). Accumulation of ^{212}Pb-rituximab in the tumour was significantly higher than that of the ^{212}Pb-isotypic control (at 6 h: 13.4 ± 1.5%ID/g versus 6.7 ± 0.3%ID/g) (Fig. 2b). Accumulation of ^{212}Pb-rituximab and ^{212}Pb-isotypic control did not differ significantly in all non-tumour tissues. Radioactivity accumulation (~10%ID/g) was observed in the spleen, liver, and in highly vascularises organs (kidneys, lungs, and heart) and was well correlated with the radioactivity in the plasma. In other organs, radioactivity was less than 5%ID/g. In vivo, SPECT-CT imaging confirmed tumour accumulation of ^{203}Pb-rituximab, similar to the BLI results in EL4-hCD20-luc cells (Fig. 2c, d). The important variability in ^{212}Pb-rituximab uptake by tumours (Fig. 2a) was related to tumour size and location variability, as observed by SPECT-CT.

Dose range finding and toxicity studies

The toxicity of 185–740 kBq ^{212}Pb-rituximab was evaluated in healthy C57BL/6 mice and compared with that induced by PBS, cold mAbs (100 µg rituximab or isotypic control), and the ^{212}Pb-isotypic control (277.5 and 555 kBq) (Fig. 3). Mice were monitored for 7 days, 21 days, or 3 months. Treatment with 555 or 740 kBq ^{212}Pb-rituximab and 555 kBq ^{212}Pb-isotypic control had toxic effects, including significant body weight loss (Supplemental Fig. 1), and 25%, 100%, and 40% of the mice, respectively, had to be euthanized within 3 weeks post-injection (Fig. 3A). Body weight loss was dose-dependent and reversible only up to 555 kBq. Activities of 185 to 370 kBq were well tolerated. Complete blood cell counts revealed haematological toxicity by ^{212}Pb-rituximab, with a similar profile as that of the ^{212}Pb-isotypic control. A significant decrease in the leucocyte count was observed starting at 185 kBq ^{212}Pb-rituximab as soon as 7 days post-injection compared with PBS ($p < 0.005$; Fig. 3Ba). The platelet count and haemoglobin concentration were also significantly reduced at 7 days after 277.5 kBq ^{212}Pb-rituximab treatment ($p < 0.005$; Fig. 3Bb, c). This haematological toxicity was partially reversible at 21 days and totally reversed at 3 months, with the exception of the haemoglobin concentration, which remained significantly lower than that in the controls. We also evaluated kidney and liver toxicities by monitoring biochemical parameters in plasma. No significant hepatic toxicity was observed, but low toxicity in the kidneys was detected at 3 months post-injection (Supplemental Fig. 2). The acute toxicity data suggested that ^{212}Pb-rituximab at 555 kBq was toxic, and that therapeutic activity should remain below this level.

RIT studies

RIT studies were performed to evaluate the therapeutic efficacy of ^{212}Pb-rituximab using a murine syngeneic lymphoma model at the early and late tumour development stages. The first efficacy study was conducted 11 days after intravenous injection of EL4-hCD20-luc cells. Survival curves are presented in Fig. 4. In the control group (PBS), a median survival time (MST) of 27 days was observed, which was not significantly different from that in the ^{212}Pb-isotypic control group (277.5 kBq, 36.5 days). All other treatments induced a significant increase in MST compared with

A

Treatment	Dose or activity	Mouse survival at end-point		
		D7	D21	M3
PBS	–	5/5	5/5	5/5
Isotypic control	100 µg	5/5	5/5	–
Rituximab	100 µg	5/5	5/5	5/5
^{212}Pb-isotypic control	277.5 kBq	5/5	5/5	5/5
	555 kBq	5/5	3/5	0/5
^{212}Pb-rituximab	185 kBq	10/10	10/10	–
	277.5 kBq	10/10	10/10	10/10
	370 kBq	10/10	10/10	10/10
	555 kBq	10/10	6/8	6/7
	740 kBq	10/10	0/10	–

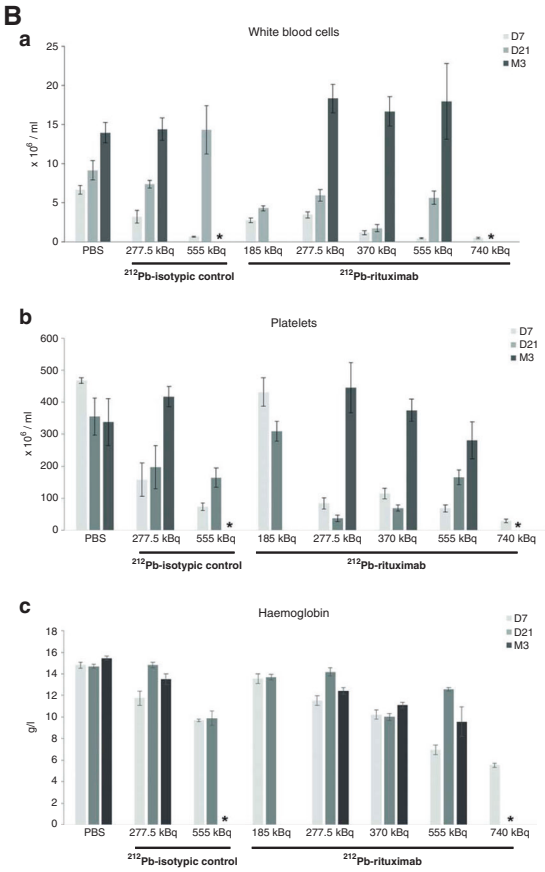

Fig. 3 Toxicity studies. A Effect of ^{212}Pb-rituximab on the survival of healthy mice. Three time points were evaluated: 7 days, 21 days, and 3 months post-injection. Values in bold indicate when lethality occurred. **B** ^{212}Pb-rituximab toxicity studies based on haematological parameters. The white blood cell count (**a**), platelet count (**b**), and haemoglobin concentration (**c**) were measured at 7 days, 21 days, and 3 months post-injection of PBS, ^{212}Pb-isotypic control (277.5 or 555 kBq), or ^{212}Pb-rituximab (185–740 kBq). Data represent the mean ± SEM. *All mice died before the endpoint.

PBS. In the 40 mg/kg rituximab (concentration used in clinical practice) group, the MST was 64 days ($p = 0.028$). The MST was not reached in the 277.5 kBq ^{212}Pb-rituximab group at the two specific activities evaluated (37 MBq/mg, $p = 0.0002$; 370 MBq/mg, $p < 0.0001$). The second efficacy study was performed 20–30 days post-intravenous injection of EL4-hCD20-luc cells once tumours were detected by BLI. Survival curves (Fig. 5) and BLI monitoring examples (Fig. 6) are shown. BLI monitoring revealed rapid tumour growth. In the control group (PBS), the MST was 9 days. Neither rituximab (40 mg/kg) nor the ^{212}Pb-isotypic control (277.5 kBq) significantly increased the MST (5 and 13 days, respectively), whereas a single ^{212}Pb-rituximab dose at 277.5 kBq on day 0 did increase significantly the MST (28 days; $p = 0.0006$). At this advanced tumour stage, a second injection of 277.5 kBq ^{212}Pb-rituximab at either 7 or 14 days after the first treatment did not significantly improve survival after a single cycle, despite a significant increase in the MST (28.5 or 29 days, respectively) compared with PBS.

DISCUSSION

Rituximab, which has been used for more than 20 years for the treatment of CD20-positive NHL, is a specific chimeric mAb targeting the CD20 surface antigen expressed on B lymphocytes, and it has considerably improved the life expectancy of NHL patients [21]. The CD20 antigen is a transmembrane phosphoprotein expressed on mature B cells and pre-B cells and is also expressed by more than 90% of B cells in NHL (but not stem cells or plasma cells). Furthermore, CD20 is not shed into the bloodstream and is not rapidly internalised. Thus, it carries many favourable attributes endorsing its use as a RIT target. Early studies using 'first generation' radiolabeled antibodies targeting CD20, such as ^{131}I-tositumomab and ^{90}Y-ibritumomab tiuxetan, induced objective tumour responses in 60–80% of patients with relapsed or refractory indolent B-cell malignancies, leading to FDA approval of both radioimmunoconjugates [3]. However, their severe side effects compared with rituximab, notably bone marrow toxicity, and their logistic challenges have limited the attractiveness of these therapeutics. α-RIT, which markedly improves cytotoxicity with a limited path length, would potentially improve the appeal of RIT, particularly in NHL, which often includes disseminated malignancies and micrometastases [6]. In this study, we evaluated ^{212}Pb-rituximab efficacy as a proof of concept of ^{212}Pb α-RIT potency. Some previous studies were performed to explore the therapeutic potential of rituximab radiolabeled with other α emitters such as ^{227}Th, ^{213}Bi, or ^{211}At [22–25]. ^{212}Pb presents certain advantages such as its easily mastered production and worldwide distribution, stable mAb radiolabeling due to the TCMC chelate, and an intermediate half-life (10.6 h), which is relatively convenient for antibody kinetics [9].

In vitro experiments showed significantly specific and dose-dependent growth inhibition, which was correlated with increased mortality, after exposure of EL4-hCD20-luc cells to ^{212}Pb-rituximab. Within 3 days, 3.7 kBq/mL ^{212}Pb-rituximab induced greater than 80% growth inhibition. This level of cytotoxicity is similar to that reported in B-lymphoma cell lines exposed to ^{211}At-rituximab [24] or ^{212}Pb-NNV003 [26] and in myeloma cell lines exposed to ^{212}Pb-daratumumab [11]. At high activity (7.4 kBq/mL), non-specific

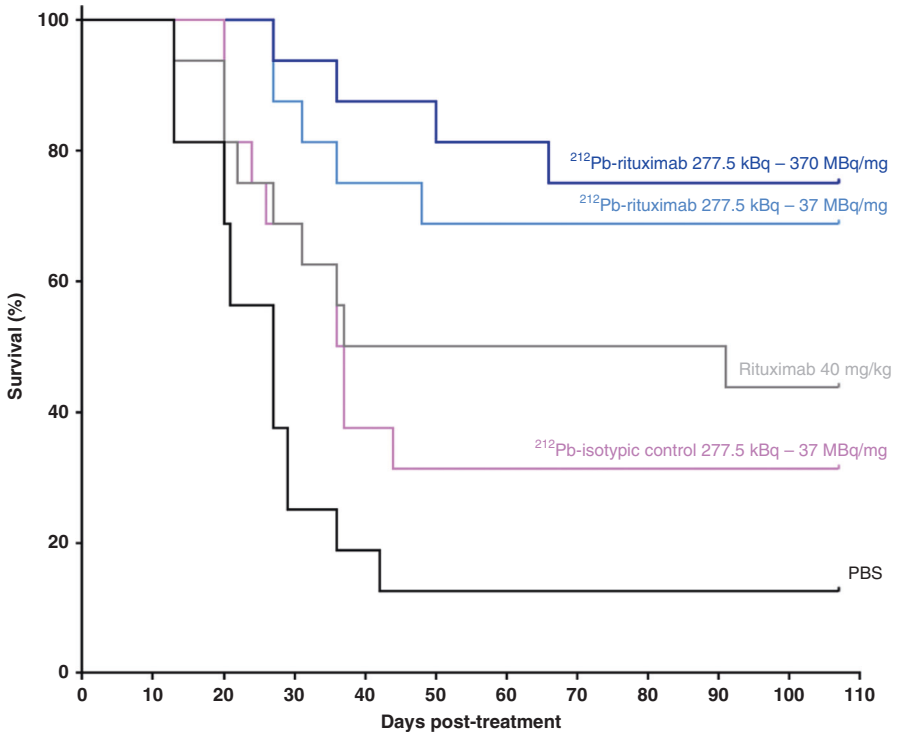

Fig. 4 Efficacy of ^{212}Pb-rituximab treatment in a murine syngeneic lymphoma model at an early stage. At 11 days post-engraftment, mice received the following treatments ($n = 16$ per group): PBS, 40 mg/kg rituximab, 277.5 kBq ^{212}Pb-isotypic control, and 277 kBq ^{212}Pb-rituximab with a specific activity of 370 MBq/mg or 37 MBq/mg. Survival rates were determined by the Kaplan–Meier method and compared using the log-rank test. All treatments except the ^{212}Pb-isotypic control induced a significant increase in MST compared with PBS.

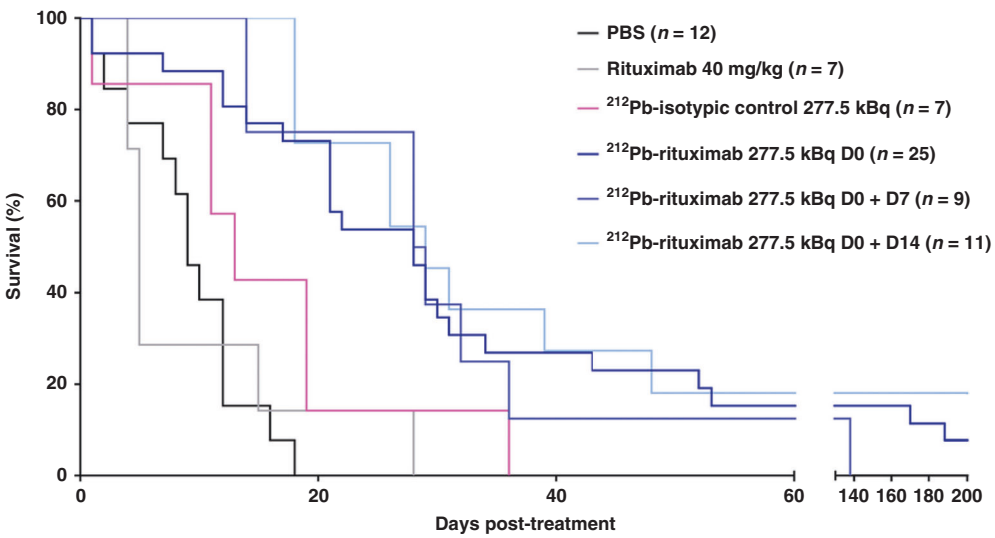

Fig. 5 Efficacy of ^{212}Pb-rituximab treatment in a late-stage murine syngeneic lymphoma model. Once the tumour was detected by BLI (20–30 days after cell injection), mice were treated with an injection of PBS, rituximab (40 mg/kg), ^{212}Pb-isotypic control (277.5 kBq), ^{212}Pb-rituximab (277.5 kBq), or two injections of ^{212}Pb-rituximab (277.5 kBq) on days 0 and 7 or days 0 and 14. Survival rates were determined by the Kaplan–Meier method and compared using the log-rank test. All ^{212}Pb-rituximab treatments induced a significant increase in the MST compared with PBS ($p \leq 0.001$).

toxicity was induced, as observed in other in vitro studies [11, 26]. This non-specific toxicity was also explained by the protocol that we have chosen, in that no washing was performed to avoid radiolabeled IgG–antigen disengagement.

^{212}Pb-rituximab post-mortem biodistribution studies in a murine syngeneic lymphoma model confirmed specific tumour uptake, with 13.4 ± 0.3%ID/g from 6 h. These studies were complemented by MicroSPECT/CT imaging using ^{203}Pb, a γ-emitter. This radioelement allowed us to consider a theranostic approach for ^{212}Pb α-therapy using a chemically identical radiometal, preventing the need for a radionuclide with different physicochemical properties, which would likely result in different pharmacokinetics. Biodistribution in non-tumour tissues revealed high initial activity levels in blood and blood-rich tissues. These results are consistent with Aurlien et al. [24], who performed biodistribution studies in Balb/c mice using ^{211}At-rituximab compared with ^{125}I-rituximab. All of these data confirm stable ^{212}Pb-rituximab radiolabeling with a very low uptake by usual

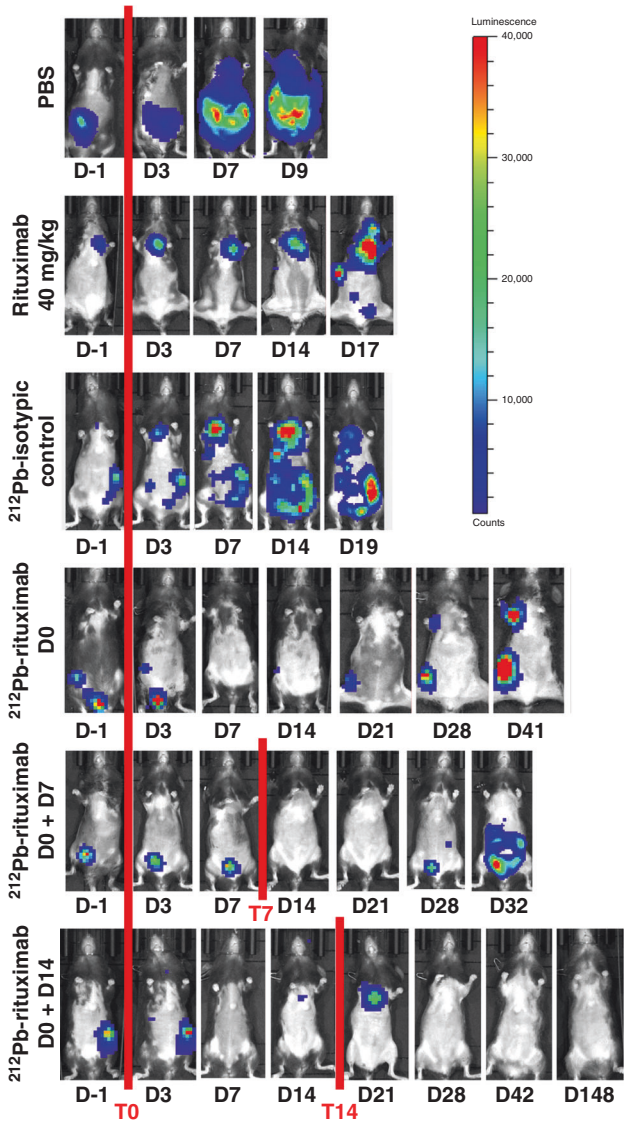

Fig. 6 BLI monitoring in a late-stage murine syngeneic lymphoma model. When the tumour was detected by BLI (20–30 days after cell injection), mice were injected with PBS, rituximab (40 mg/kg), ^{212}Pb-isotypic control (277.5 kBq), ^{212}Pb- rituximab (277.5 kBq) on day 0 (T0), or ^{212}Pb-rituximab (277.5 kBq) on T0 and day 7 (T7) or T0 and day 14 (T14). Mice were monitored by BLI at the indicated time points to follow tumour evolution until sacrifice or the end of the experiment.

lead-fixing organs (e.g., bone). Furthermore, tissue accumulation suggests that the spleen, kidneys, and lung could be toxicity-limiting organs. These biodistribution results are similar to results of Maaland et al. with ^{212}Pb-NNV003 who obtained the same list of organs at risk [26].

Toxicity studies revealed partial survival at 555 kBq ^{212}Pb-rituximab and 100% lethality at 740 kBq ^{212}Pb-rituximab before 21 days. This range of toxic activity is very close to that reported in the study by Maaland using ^{212}Pb-NNV003 [26]. Haematological data showed dose-dependent bone marrow suppression with a decrease in all blood cell lineages using ^{212}Pb-rituximab, but this effect was not significantly different from that induced by an irrelevant antibody. Haematological toxicity is correlated with the presence of high levels of radioactivity in the bloodstream. As rituximab have a low affinity to murine CD20, this study probably underevaluated a potential haematological toxicity in human. Haematological toxicity at high activity is responsible of acute toxicity limiting dose correlated with weight loss, but at activity lower than 555 kBq, this toxicity is reversible. A full recovery of white blood cells was observed at 3 months, even at the 555 kBq dose, whereas anaemia persisted because of a slower turnover of red blood cells. Furthermore, biochemical data showed short-term treatment safety in the liver and kidneys but possibly long-term (3 months) toxicity in the kidneys. This dose range finding study allow us to determine a safety activity (277.5 kBq ^{212}Pb-rituximab) to perform therapy studies. Nevertheless, to further improve tumour biodistribution and reduce toxicity, preloading with an anti-CD20 antibody before RIT could be an interesting alternative, as was done for ^{90}Y-ibritumomab tiuxetan, whereby a standard dose of rituximab was administered before RIT. Kletting et al. [27] showed that for optimal results, preloading dosages can be personalised particularly in terms of the tumour uptake index. This therapeutic optimisation could be possible for ^{212}Pb with the help of SPECT/CT imaging using ^{203}Pb. Imaging might enable evaluation of patient-specific dosimetry and the patient's response to ^{212}Pb-targeted therapy. Thus, ^{212}Pb treatment could be combined with ^{203}Pb for a theranostic approach, which represents an emerging strategy [28–30].

Efficacy studies were performed in a murine syngeneic lymphoma model. The tumour model developed by intravenous injection of EL4-hCD20-luc cells has the advantage of being in an immunocompetent mouse. Moreover, tumour development in mice mimics tumour development in humans with a large variability in tumour sites such as cervical, inguinal, axillar, retroperitoneal and mediastinal lymph nodes, or the spleen. This variability is highlighted by BLI and SPECT/CT data.

Efficacy studies showed that ^{212}Pb-rituximab treatment significantly prolonged the MST compared with PBS, rituximab (40 mg/kg), or the ^{212}Pb-isotypic control. The treatment was tested on two time points: 11 and 20–30 days post-intravenous injection of EL4-hCD20-luc. At 11 days, the tumours were not detectable by BLI, and the stage of tumour development corresponded to micrometastases. At this tumour stage, survival was near 75% in mice treated with ^{212}Pb-rituximab groups at over 3 months post-treatment with a single cycle regimen, compared with ~10% survival in the PBS group. Two specific activities were tested, but no significant difference was observed between them in terms of therapeutic efficacy. Our observations are comparable with those in NHL treated with ^{212}Pb-NNV003, an anti CD37 antibody [26], and in multiple myeloma treated with ^{212}Pb-daratumumab, an anti-CD38 antibody [11]. In those studies, 90–280 kBq ^{212}Pb-NNV003 was effective and safe when administered 2 days after intravenous injection of Daudi cells. Similarly, 185–277.5 kBq ^{212}Pb-daratumumab significantly increased survival in a mouse myeloma xenograft model.

The MST was also significantly increased in mice treated with ^{212}Pb-rituximab at the time of tumour detection by BLI (28 vs. 9 days in the PBS group), indicating that even under a high tumour burden, ^{212}Pb-rituximab was still somewhat efficient. In mice with high tumour burdens, a second administration of ^{212}Pb-rituximab was performed but did not further improve efficacy. Complementary investigations should be performed to evaluate fractionated regimens. For example, in midgut neuroendocrine tumours, ^{177}Lu-Dotatate was injected four times at 8-week intervals [31].

In theory, due to their short range and high level of cytotoxicity, α-particles are more suitable than β-particles for the treatment of disseminated lymphoma disease. Several RIT preclinical and clinical studies have been performed to evaluate rituximab coupled to a β-emitter (^{90}Y, ^{131}I, and ^{177}Lu) [3, 32]. A preclinical study using ^{177}Lu-rituximab was performed in nude Balb/c mice grafted with Raji cells. Even if β-RIT induced significant tumour regression, no tumour disappearance was observed [32]. Our study confirms the high anti-tumour ability of α-emitters.

To further optimise ^{212}Pb-rituximab efficacy and enhance the ratio of tumour to normal organ irradiation, innovative approaches using pre-targeting or smaller mAb fragments can be investigated [4, 33].

In conclusion, the data obtained in this study and other studies of ^{212}Pb-rituximab efficacy are promising and highlight the potency of ^{212}Pb-RIT in NHL and the potential of α-RIT in general.

Reporting summary

Further information on research design is available in the Nature Research Reporting Summary linked to this article.

DATA AVAILABILITY

The datasets used and/or analysed during the current study are available from the corresponding author on reasonable request.

REFERENCES

1. Shankland KR, Armitage JO, Hancock BW. Non-Hodgkin lymphoma. Lancet. 2012;380:848–57.
2. Beers SA, Chan CHT, French RR, Cragg MS, Glennie MJ. CD20 as a target for therapeutic type I and II monoclonal antibodies. Semin Hematol. 2010;47:107–14.
3. Witzig TE. Radioimmunotherapy for B-cell non-Hodgkin lymphoma. Best Pract Res Clin Haematol. 2006;19:655–68.
4. Eskian M, Khorasanizadeh M, Zinzani PL, Illidge TM, Rezaei N. Novel methods to improve the efficiency of radioimmunotherapy for non-Hodgkin lymphoma. Int Rev Immunol. 2019;38:79–91.
5. Baidoo KE, Yong K, Brechbiel MW. Molecular pathways: targeted α-particle radiation therapy. Clin Cancer Res. 2013;19:530–7.
6. Jurcic JG. Targeted alpha-particle therapy for hematologic malignancies. Semin Nucl Med. 2020;50:152–61.
7. Kim Y-S, Brechbiel MW. An overview of targeted alpha therapy. Tumour Biol. 2012;33:573–90.
8. Nelson BJB, Andersson JD, Wuest F. Targeted alpha therapy: progress in radionuclide production, radiochemistry, and applications. Pharmaceutics. 2020;13:49.
9. Yong K, Brechbiel MW. Towards translation of 212Pb as a clinical therapeutic; getting the lead in! Dalton Trans. 2011;40:6068–76.
10. Chappell LL, Dadachova E, Milenic DE, Garmestani K, Wu C, Brechbiel MWSynthesis. characterization, and evaluation of a novel bifunctional chelating agent for the lead isotopes 203Pb and 212Pb. Nucl Med Biol. 2000;27:93–100.
11. Quelven I, Monteil J, Sage M, Saidi A, Mounier J, Bayout A, et al. 212Pb Alpha-radioimmunotherapy targeting CD38 in multiple myeloma: a preclinical study. J Nucl Med. 2019;61:1058–65.
12. Meredith RF, Torgue J, Azure MT, Shen S, Saddekni S, Banaga E, et al. Pharmacokinetics and imaging of 212Pb-TCMC-trastuzumab after intraperitoneal administration in ovarian cancer patients. Cancer Biother Radiopharm. 2014;29:12–7.
13. Meredith RF, Torgue JJ, Rozgaja TA, Banaga EP, Bunch PW, Alvarez RD, et al. Safety and outcome measures of first-in-human intraperitoneal α radioimmunotherapy with 212Pb-TCMC-trastuzumab. Am J Clin Oncol. 2018;41:716–21.
14. Daydé D, Ternant D, Ohresser M, Lerondel S, Pesnel S, Watier H, et al. Tumor burden influences exposure and response to rituximab: pharmacokinetic-pharmacodynamic modeling using a syngeneic bioluminescent murine model expressing human CD20. Blood. 2009;113:3765–72.
15. Langford DJ, Bailey AL, Chanda ML, Clarke SE, Drummond TE, Echols S, et al. Coding of facial expressions of pain in the laboratory mouse. Nat Methods. 2010;7:447–9.
16. Jeger S, Zimmermann K, Blanc A, Grünberg J, Honer M, Hunziker P, et al. Site-specific and stoichiometric modification of antibodies by bacterial transglutaminase. Angew Chem Int Ed Engl. 2010;49:9995–7.
17. Dennler P, Chiotellis A, Fischer E, Brégeon D, Belmant C, Gauthier L, et al. Transglutaminase-based chemo-enzymatic conjugation approach yields homogeneous antibody-drug conjugates. Bioconjug Chem. 2014;25:569–78.
18. Carpenet H, Cuvillier A, Monteil J, Quelven I. Anti-CD20 immunoglobulin G radiolabeling with a 99mTc-tricarbonyl core: in vitro and In vivo evaluations. PLoS ONE. 2015;10:e0139835.
19. FDA. Clinical review of BLA reference NO. BLA 97–0260 AND BLA 97–0244. 1997 - U.S. Food and Drug Administration Search Results.
20. van der Have F, Vastenhouw B, Ramakers RM, Branderhorst W, Krah JO, Ji C, et al. U-SPECT-II: an ultra-high-resolution device for molecular small-animal imaging. J Nucl Med. 2009;50:599–605.
21. Coiffier B, Haioun C, Ketterer N, Engert A, Tilly H, Ma D, et al. Rituximab (anti-CD20 monoclonal antibody) for the treatment of patients with relapsing or refractory aggressive lymphoma: a multicenter phase II study. Blood. 1998;92:1927–32.
22. Dahle J, Borrebæk J, Jonasdottir TJ, Hjelmerud AK, Melhus KB, Bruland ØS, et al. Targeted cancer therapy with a novel low-dose rate α-emitting radioimmunoconjugate. Blood. 2007;110:2049–56.
23. Park SI, Shenoi J, Pagel JM, Hamlin DK, Wilbur DS, Orgun N, et al. Conventional and pretargeted radioimmunotherapy using bismuth-213 to target and treat non-Hodgkin lymphomas expressing CD20: a preclinical model toward optimal consolidation therapy to eradicate minimal residual disease. Blood. 2010;116:4231–9.
24. Aurlien E, Larsen RH, Kvalheim G, Bruland OS. Demonstration of highly specific toxicity of the alpha-emitting radioimmunoconjugate (211)At-rituximab against non-Hodgkin's lymphoma cells. Br J Cancer. 2000;83:1375–9.
25. Green DJ, Shadman M, Jones JC, Frayo SL, Kenoyer AL, Hylarides MD, et al. Astatine-211 conjugated to an anti-CD20 monoclonal antibody eradicates disseminated B-cell lymphoma in a mouse model. Blood. 2015;125:2111–9.
26. Maaland AF, Saidi A, Torgue J, Heyerdahl H, Stallons TAR, Kolstad A, et al. Targeted alpha therapy for chronic lymphocytic leukaemia and non-Hodgkin's lymphoma with the anti-CD37 radioimmunoconjugate 212Pb-NNV003. PLoS ONE. 2020;15:e0230526.
27. Kletting P, Meyer C, Reske SN, Glatting G. Potential of optimal preloading in anti-CD20 antibody radioimmunotherapy: an investigation based on pharmacokinetic modeling. Cancer Biother Radiopharm. 2010;25:279–87.
28. Pandit-Taskar N. Targeted radioimmunotherapy and theranostics with alpha emitters. J Med Imaging Radiat Sci. 2019;50:S41–4.
29. Dos Santos JC, Schäfer M, Bauder-Wüst U, Lehnert W, Leotta K, Morgenstern A, et al. Development and dosimetry of 203Pb/212Pb-labelled PSMA ligands: bringing « the lead » into PSMA-targeted alpha therapy? Eur J Nucl Med Mol Imaging. 2019;46:1081–91.
30. Banerjee SR, Minn I, Kumar V, Josefsson A, Lisok A, Brummet M, et al. Preclinical evaluation of 203/212Pb-labeled low-molecular-weight compounds for targeted radiopharmaceutical therapy of prostate cancer. J Nucl Med. 2020;61:80–8.
31. Strosberg J, El-Haddad G, Wolin E, Hendifar A, Yao J, Chasen B, et al. Phase 3 trial of ^{177}Lu-dotatate for midgut neuroendocrine tumors. N. Engl J Med. 2017;376:125–35.
32. Wojdowska W, Karczmarczyk U, Balog L, Sawicka A, Pósténvi Z, Kovács-Haász V, et al. Impact of DOTA-chelators on the antitumor activity of 177Lu-DOTA-rituximab preparations in lymphoma tumor-bearing mice. Cancer Biother Radiopharm. 2020;35:558–62.
33. Krasniqi A, D'Huyvetter M, Xavier C, Jeught KV, der, Muyldermans S, Heyden JVD, et al. Theranostic radiolabeled anti-CD20 sdAb for targeted radionuclide therapy of non-Hodgkin lymphoma. Mol Cancer Ther. 2017;16:2828–39.

ACKNOWLEDGEMENTS

CRIBL is member of the Consortium for the Acceleration of Innovation and its Transfer in the Lymphoma Field (CALYM) Carnot Institute www.calym.org. We would also like to thank Dr. Jeanne Cook-Moreau for proofreading and our radiation protection officer, Dr. Eric Pinaud.

AUTHOR CONTRIBUTIONS

SDP, JM, AS, JT, MiC and IQ conceptualised the study; SDP and IQ assembled, analysed and interpreted data, and wrote the manuscript; MS, AG and MaC performed experiments and collected the data; JM and IQ performed SPECT/CT imaging treatment; AS, JT and MiC helped with manuscript preparation.

FUNDING

This research was supported by BPI France.

COMPETING INTERESTS

Amal Saidi and Julien Torgue are Orano Med employees. No other potential conflicts of interest relevant to this article exist.

ETHICS APPROVAL AND CONSENT TO PARTICIPATE

All applicable international, national and institutional guidelines for the care and use of animals were followed. This article does not contain any studies with human participants performed by any of the authors.

CONSENT TO PUBLISH

Not applicable.

ADDITIONAL INFORMATION

Supplementary information The online version contains supplementary material available at https://doi.org/10.1038/s41416-021-01585-6.

Correspondence and requests for materials should be addressed to Michel Cogne or Isabelle Quelven.